ADVANCED MATERIALS
www.advmat.de

Topology and Symmetry in Quantum Materials

Bahadur Singh, Hsin Lin, and Arun Bansil*

Interest in topological materials continues to grow unabated in view of their conceptual novelties as well as their potential as platforms for transformational new technologies. Electronic states in a topological material are robust against perturbations and support unconventional electromagnetic responses. The first-principles band-theory paradigm has been a key player in the field by providing successful prediction of many new classes of topological materials. This perspective presents a cross section through the recent work on understanding the role of geometry and topology in generating topological states and their responses to external stimuli, and as a basis for connecting theory and experiment within the band theory framework. In this work, effective strategies for topological materials discovery and impactful directions for future topological materials research are also commented.

1. Introduction

Advanced materials with their unique properties lie at the heart of the current condensed matter research.[1–7] In crystalline materials, the band theory framework has provided a natural language for organizing the electronic states. Translational invariance of crystals allows the eigenstates to be classified in terms of the crystal momentum k in the periodic Brillouin zone (BZ), and the associated Bloch wavefunctions u_{nk} with energies E_{nk}, where n is the band index.[8] Practical calculations of the energy spectrum (band structure) in crystals widely rely on the framework of the density functional theory (DFT), and the continuing development of ever more accurate exchange-correlation functionals.[9–12]

Importance of geometric properties of the Bloch states and the constraints imposed on the band structure through the underlying crystalline and non-crystalline symmetries have been well recognized in materials. For example, symmetries often dictate degeneracies at high-symmetry points in the BZ. The role of geometric properties in driving novel phenomena was highlighted by the breakthrough discovery of topological states in 2D and 3D materials where these unique states were found to emerge when a gap in the electronic spectrum narrows, closes and reopens "inverted" from its natural order under spin-orbit coupling (SOC) effects.[13–17] Topology of states can be characterized via the associated topological invariants, which are global indices related to the geometry of the wavefunctions in momentum space.[17–24] A nontrivial topological number guarantees the existence of robust surface/edge states that are insensitive to smooth changes in material parameters, much like the basic shape or topology of an object that remains intact under smooth deformations. The appearance of topological states in a material reflects the presence of a nontrivial topology of the electronic wavefunctions. The best-known example is that of the quantum Hall state (QHS) of electrons in 2D subjected to a strong magnetic field.[25] The QHS is electrically insulating in the bulk, but it supports chiral conducting states along its boundary that cannot be eliminated without destroying the associated bulk state. QHS has provided the most precise standard for resistivity and for the determination of the fine structure constant.[25,26]

Topological materials research is concerned with characterizing and manipulating the properties of materials by exploiting the topology and symmetry of electronic states in the reciprocal as well as the real space. In this way, many topologically interesting materials that host unique properties have been identified. These include Z_2 strong/weak topological insulators, topological crystalline insulators, higher-order topological insulators, Dirac, Weyl, nodal, and multifold semimetals, among other possibilities.[2–7] Many of these theorized states have been verified by identifying their nontrivial states via angle-resolved photoemission and scanning-tunneling spectroscopy experiments. Interestingly, the low-energy excitations harbored by topological materials mimic the elementary relativistic particles, which have traditionally been the domain of high-energy physics. Topological materials thus provide a fertile ground for cross-pollination of ideas across high- and low-energy physics and a rich setting for exploring quantum phenomena involving Weyl, Dirac, Majorana, and axion states on a far more accessible solid-state materials platform with unprecedented opportunities for investigating fundamental science questions and developing next-generation applications.[27–32]

The band theory paradigm has often guided the related experimental work through reliable prediction of new topological materials and the validation of their striking quantized properties

B. Singh
Department of Condensed Matter Physics and Materials Science
Tata Institute of Fundamental Research
Mumbai 400005, India
E-mail: bahadur.singh@tifr.res.in
H. Lin
Institute of Physics
Academia Sinica
Taipei 11529, Taiwan
A. Bansil
Department of Physics
Northeastern University
Boston, Massachusetts 02115, USA
The ORCID identification number(s) for the author(s) of this article can be found under https://doi.org/10.1002/adma.202201058.

DOI: 10.1002/adma.202201058

via spectroscopy and transport experiments. This requires an extension of the familiar framework of band structure computations to include an overlayer of analysis of topological invariants resulting from considerations of topology and crystalline symmetries.[2,3] The advances in band theory combining topology and crystalline symmetries have allowed a broad classification of topological states. In particular, the insulating nonmagnetic materials covered by 230 space groups have been shown to support ≈3000 possible choices.[22] We emphasize that while the existence of the allowed topological states can be inferred from symmetry considerations, their numbers, energy dispersions, and geometries depend on details of the surfaces and edges involved, demanding an in-depth material-specific modeling effort. Recent progress in topological quantum chemistry and symmetry characterization techniques has enabled high-throughput analysis of topology in large classes of experimentally realized 2D and 3D materials, indicating that about half of the existing stoichiometric nonmagnetic materials are topologically nontrivial.[33–36] Experimental validation, however, has proven challenging, and it is currently limited to a small number of materials due, in part, to the fact that most materials do not present clean nontrivial states at the charge neutrality point even in their pristine form. New design strategies using existing materials or bottom-up synthesis should help realize new topologically interesting materials that are stable under ambient conditions.

2. Diagnosing Band Topology

Topology has emerged as the fundamental organizing principle for characterizing quantum states. The associated topological invariants reflect the geometry (or winding) of the electronic wavefunction in k space and depend on the symmetry group of the crystal lattice. These invariants control the quantized responses of the material and remain preserved under adiabatic tunings of the Hamiltonian that do not change its symmetry group. Intuitively, a topologically nontrivial state can be envisioned to emerge from a band inversion in which the valence and conduction bands switch order at specific high-symmetry k points near the Fermi level from their natural order in the atomic limit, see **Figure 1**a. The inversion of Bi and Se 5p states at the Γ point in Bi_2Se_3 under SOC effects is a prominent example (Figure 1b). The band inversion can, in principle, involve any pair of states with different orbital and magnetic quantum numbers. Although all topologically nontrivial states can be identified, at least heuristically, via the band-inversion scenario, quantitative analyses are needed to pin down details of their emergence from the atomic limit.[2,3]

Three different approaches have been used widely to ascertain the topological states of materials as follows: 1) Direct computation of topological invariants and symmetry indicators.[20–24] 2) Use of adiabatic continuation to connect the topological state of an unknown material to that of a known material.[37] And 3) invoking the bulk-boundary correspondence based on a direct computation of the boundary states.[38,39] The first two approaches require analysis of symmetry properties of the bulk states, which are encoded in their irreducible representations at the high-symmetry points in the BZ. Such a characterization was envisaged initially as a parity criterion in inversion-symmetric insulators,[17] which was generalized later to encompass all space groups.[20–22] The third approach uncovers the nontrivial states through their connections with the bulk bands and serves also to identify experimentally accessible fingerprints for affirming the nontrivial nature of a material.

3. Topological States in Insulators

Insulators present a fundamental ground state of solids that is electrically inert because an energy gap separates their occupied and unoccupied states.[40] Topological insulators (TIs) are a new type of insulator where the material possesses a bulk bandgap, but it can still conduct electricity via its robust spin-polarized metallic states that emerge on its surface owing to the nontrivial winding of the bulk states.[41–45] We can understand the nature of the electronic spectrum of a TI by considering band structures without and with SOC effects. Let us assume that without the SOC, the system is a topologically trivial insulator or a metal/semimetal. If we now track the evolution of states near the Fermi energy, we can easily envision a topological phase transition from a trivial to a nontrivial state via a band inversion induced by scaling the strength of the SOC.[45–49] The gap must close at a critical point that lies between the two topologically distinct states. Topology of the material remains unchanged as long as the bulk energy gap and its topological character remains intact under variations in the Hamiltonian (Figure 1a). Notably, the surfaces/edges of a TI act as an interface between the nontrivial bulk and the trivial vacuum, and the bulk-boundary correspondence then yields the protected gapless (metallic) surface states that connect the filled and unfilled bulk states (Figure 1a,b).

TIs are described by a Z_2 topological invariant that is defined in the presence of time-reversal symmetry $\Theta^2 = -1$ for spinful systems.[16,17] Here, Z_2 can take two values, 0 and 1, which describe topologically trivial and nontrivial cases, respectively. For the spinless case, the time-reversal operator is $\Theta^2 = 1$, so that the system is Z_2 trivial without the SOC. Value of Z_2 can be obtained from the bulk electronic states by calculating the inversion eigenvalues of the occupied bands at the time-reversal-invariant momentum (TRIM) points, or by using the more general method of Wannier charge-center evolution,[17,23,24] which traces the evolution of the Berry phase of the valence bands between the TRIM points.[50] The nontrivial Z_2 number also manifests itself in the surface energy spectrum in that an odd number of surface states connect the bulk valence and conduction bands in the nontrivial case. The surface states of TIs exhibit linear energy dispersions around the TRIM points, like the massless Dirac equation in two dimensions. These surface states are protected by time-reversal symmetry and possess a helical spin texture wherein spin is locked perpendicular to momentum.[44,46] Topological surface states are not allowed to backscatter in the absence of magnetic impurities or other time-reversal breaking perturbations (Figures 1c,d).

Following the initial prediction of protected edge and surface states in graphene and HgTe/CdTe quantum well systems,[41,42] many classes of materials have been predicted theoretically to host the TI state through explicit calculations of the Z_2

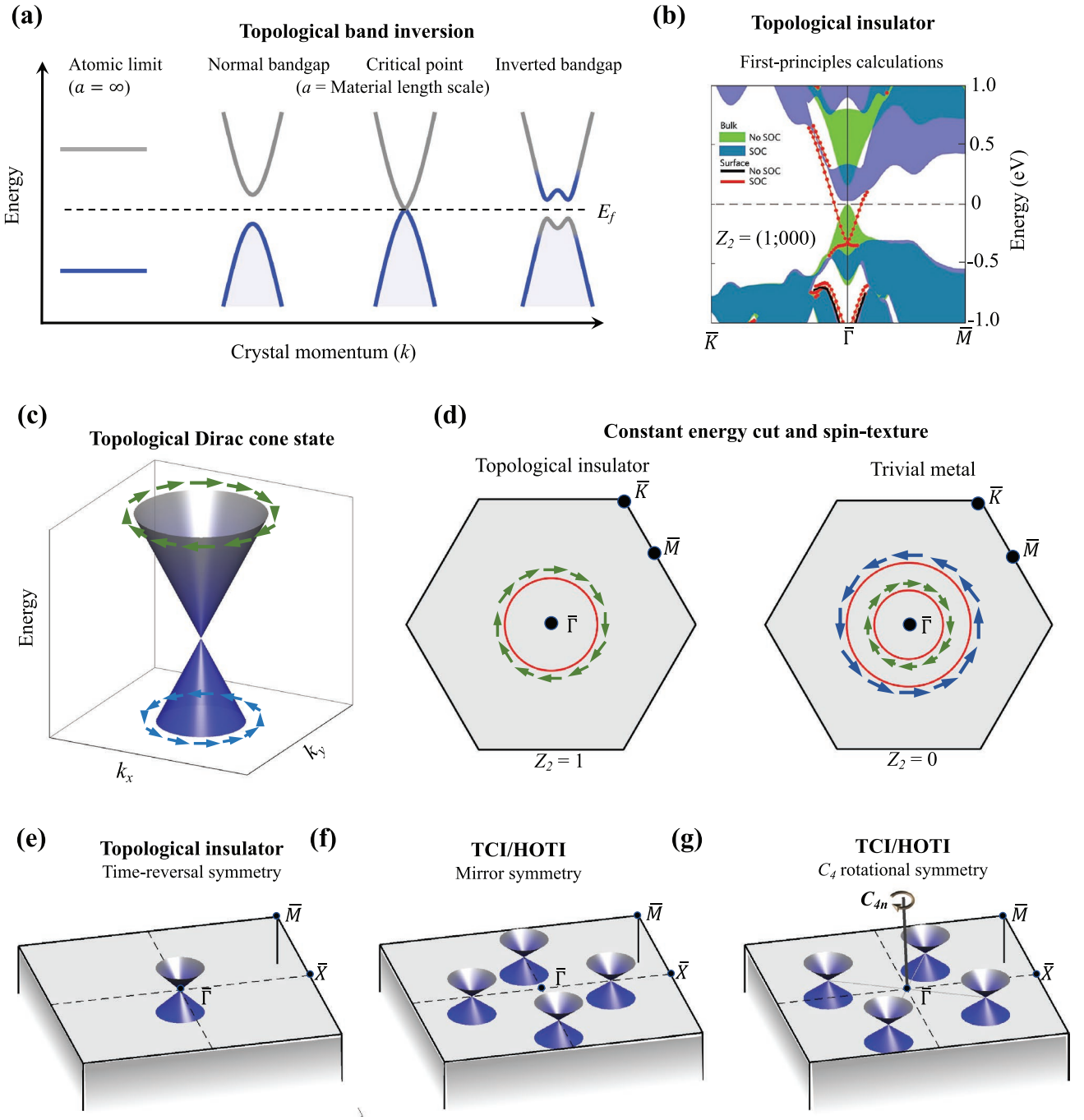

Figure 1. Band inversion and topology in insulators. a) Energy levels in the atomic limit provide the natural order of the occupied (blue line) and empty (gray line) orbitals. As the lattice parameter (a) decreases, the gap between the occupied and unoccupied Bloch states decreases and closes at a critical value of a and then reopens inverted with respect to the atomic order, realizing a topological state. b) Band structure of the Z_2 topological insulator (TI) Bi_2Se_3. Shaded regions mark bulk bands projected over the surface BZ. Dotted lines identify surface bands. Bulk-band ordering is normal without spin-orbit coupling (green shading), but it becomes inverted (blue shading) when spin-orbit coupling in included. Gapless surface states (dotted red lines) emerge (with spin-orbit coupling OC) in the bulk band gap with the Dirac node lying at the $\bar{\Gamma}$ point below the E_f. c) Schematic of spin nondegenerate energy-momentum dispersion of nontrivial surface states in TIs, which form 2D Dirac cones. Spin and momentum of these states are locked perpendicular to each other, realizing a helical spin texture with opposite helicities in the upper and lower cones. d) The spin-polarized constant energy surfaces associated with the surface states of a TI consist of a single contour, while those in a conventional metal involve two contours. An electronic orbit encircling the constant energy surfaces in a TI carries a Berry phase of π, the corresponding phase for a trivial metal is zero. e–g) Nontrivial surface states in various classes of TIs. e) A single Dirac cone pinned at a time-reversal-invariant momentum point as in Bi_2Se_3 TI. f) Four Dirac cones pinned on the projected mirror-symmetry lines (dashed) in a mirror-protected topological crystalline insulator; the mirror Chern number here is $C_M = |2|$. g) Four Dirac cones lying on the surface normal to C_4 rotational axis in a C_4 rotational-symmetry-protected topological crystalline insulator. Panel (b) reprinted with permission from Ref. [43] Springer Nature Limited.

invariants and surface state spectra. Examples include Bi_2Se_3,[45] $TlBiSe_2$ class of semiconductors,[47,51] tetradymite-like layered materials with general chemical formulas B_2X_2X', AB_2X_4, $A_2B_2X_5$, and AB_4X_7 (A = Pb, Sn, Ge; B = Bi, Sb; X, X' = S, Se, or Te),[48,52] ternary half-Heusler compounds,[53,54] Li_2AgSb class semiconductors,[37] among other materials.[2] Early predictions of TIs in materials involving heavier atoms have been extended to include materials with lighter atoms where the band inversion is driven by modulating the crystal structure through external controls of strain, pressure, alloying, charge confinement, and electric field.[46–49] The TI state has also been identified in correlated materials displaying a variety of effects such as the Kondo effect, superconductivity, magnetism, and ferroelectricity.[55–60]

Insulators with an even number of bulk band inversions are further characterized as weak TIs[17,61,62] or topological crystalline insulators (TCIs).[63,64] Weak TIs can be considered as stacked 2D TIs (or quantum spin Hall insulators) where 2D Dirac states lie only on specific crystal surfaces of the 3D system. Band inversions in weak TIs usually involve two distinct TRIM points in the BZ. This is the case, for example, in Bi_2TeI in which band inversions occur at the Γ and Z points.[61] The weak TI state has been recently verified through ARPES experiments in quasi-1D β –Bi_4I_4;[62] -the surface Dirac cone is seen on the (100) side surface but not on the top (001) surface. The TCI state is a natural extension of a Z_2 TI in which topological states are protected by symmorphic or nonsymmorphic crystalline symmetries.[63,64] The nontrivial topology in a TCI is featured via the presence of an even number of topological states on a suitable surface/hinge of the material (Figure 1e–g). The topological invariant to identify a TCI is a Z-value Chern invariant that can be evaluated by either calculating the symmetry-based indicators or the Wannier charge centers on symmetry protecting planes.[63–66] The first experimentally realized TCI is SnTe where the nontrivial state is protected by a mirror-plane symmetry with mirror Chern number 2 (Figure 1f).[67–69] The even number of Dirac-cone surface states in SnTe have been verified on the crystal surfaces symmetric with [110] mirror planes. Recently, SrPb has been confirmed as the first twofold rotational symmetry C_{2y}-protected TCI with rotational invariant 2.[70] Here, two gapless Dirac cone surface states are observed lying on the (010) surface via angle-resolved spectroscopy measurements. Many other proposed TCIs still await experimental confirmation.[65,66] The TCIs are also related to higher-order topological insulators (HOTIs) where the symmetry-protected states exist at the hinges of the surface. This possibility arises when the symmetry-protected facets are not normal to crystalline surfaces but pass through the hinges of the surface.[71–74] In this case, the surface states are gapped out and helical hinge states emerge on the mirror-protected lines.

Magnetic materials provide a natural playground for exploring the interplay between band topology and electronic correlations. TI states in magnetic insulators exhibit unique features.[75] A prominent example is the quantum anomalous Hall state (QAHS) in which the 1D chiral edge state appears in the inverted 2D bandgap created by the internal magnetism of the material. QAHS is described by a Chern invariant that can be obtained by calculating the Berry flux associated with the occupied Bloch states in the full BZ. The first experimental verification of a QAHS was reported in Cr-doped (Bi, Sb)$_2$Te$_3$ thin-films where a gate-tuned quantum anomalous Hall conductance of e^2h^{-1} was observed at low temperatures.[76] The search for magnetic materials with large inverted bandgaps and the high associated operating temperatures leads naturally to 3D magnetic TIs and axion insulators.[77–83] The topological state of centrosymmetric magnetic materials with broken time-reversal symmetry can be identified by an additional parity-based indicator Z_4.[77,78] The Z_4 topological invariant can take two values, 0 and 2 for topologically trivial and nontrivial insulators, respectively (Z_4 = 1 and 3 correspond to nontrivial metals). Nontrivial topological magnetic insulators support an axion insulator state with a quantized topological magnetoelectric effect. Surfaces of axion insulators display a half-integer quantum Hall effect if their surface states are gapped.[30] Intrinsic nontrivial magnetic insulators (antiferromagnetic and ferromagnetic) have been identified recently in natural heterostructure $MnBi_{2n}Te_{3n+1}$ (n = 1, 2, 3, and 4)[80–83] and $EuIn_2As_2$ with novel electromagnetic responses.[77,78]

4. Topological States in Semimetals

Semimetals host a vanishing densities of states at the Fermi energy and lack a global bandgap in the bulk energy spectrum. There are two distinct mechanisms for realizing a semimetal. In the first case, the valence and conduction band extrema are located at different k points in the BZ with a small overlap in energy. Such semimetals possess a local bandgap everywhere in the BZ and are adiabatically connected to the insulators. For this reason, they are loosely considered as insulators in the context of topological band theory, and their characterization follows along the lines of the TIs. TIs such as Bi_xSb_{1-x},[44] $TaAs_2$ materials,[84] ZrPtGe,[85] and other materials[86,87] belong to this class of semimetals with electron-hole pockets at the Fermi energy.

In the second case, the bulk valence and conduction bands meet at a few isolated k points in the BZ but otherwise remain separated in energy, see **Figure 2**. These semimetals are broadly referred to as nodal-point semimetals.[4,7] Spinless graphene is a famous example in 2D where the valence and conduction bands cross at the K symmetry points in the hexagonal BZ to realize the Dirac nodes. Energy dispersion around these nodes is linear in momentum and described by the 2D Dirac equation.[88] The Weyl[51,89–94] and Dirac semimetals[89,95–101] are the 3D analogs of graphene where the energy dispersion is linear in momentum along all three directions. The low-energy excitations near the band-touching points in Weyl and Dirac semimetals are described by the celebrated Weyl and Dirac equations of high-energy physics.[102,103] In Weyl semimetals, the band-touching points (Weyl nodes) are both the sources and the sinks of the Berry curvature field in momentum space. The integral of the Berry curvature field on a surface that encloses a Weyl node is a quantized integer that defines the topological charge or Chern number associated with the node. The Weyl nodes always come in pairs of opposite charges due to constraints of the Nielsen–Ninomiya no-go theorem.[104] Projections of Weyl nodes on BZ surfaces are connected via nontrivial Fermi-arc surface states. Notably, a plane cutting through the bulk Weyl nodes presents

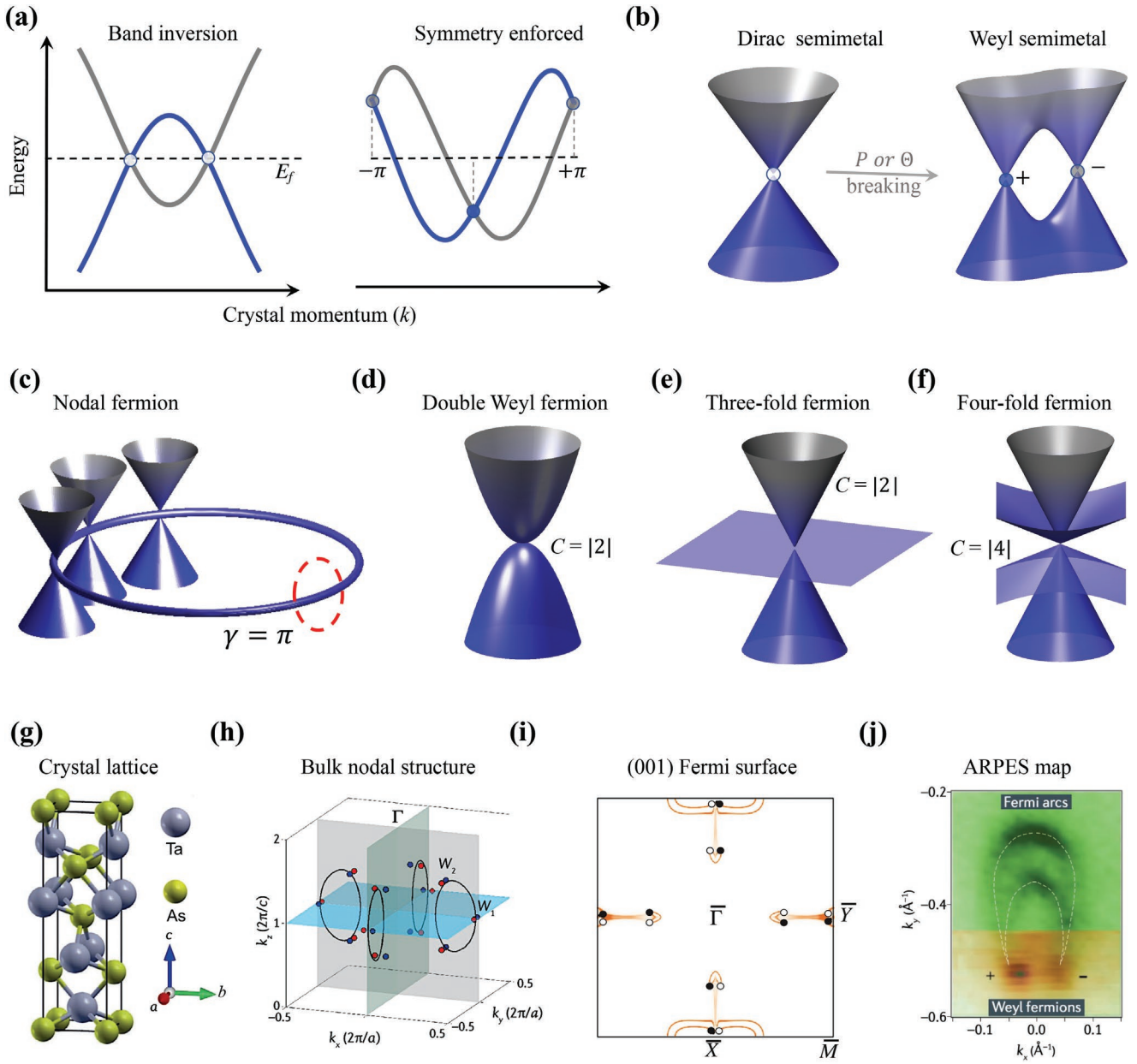

Figure 2. Classification of topological states in semimetals. a) Topological semimetals can be generated through bulk band inversions in materials. The inverted valence and conduction band crossings are protected by a crystalline rotational or mirror symmetry (left). The crossing points are four-fold degenerate in Dirac semimetals and protected by rotational symmetry in the presence of inversion (P) and time-reversal (Θ) symmetries. The band crossings are two-fold degenerate in Weyl semimetals and form chiral Weyl fermions separated in momentum space, where the distance between the oppositely charged Weyl nodes protects the Weyl semimetal phase. Topological semimetals are formed without a bulk band inversion in the case of a Kramers–Weyl fermion or nonsymmorphic semimetals (right). Here, the nonsymmorphic crystal symmetries protect the band crossings generated by spin-orbit coupling. Classification of topological semimetals based on the degeneracies and energy-momentum relationships near the band touching points. b) A fourfold degenerate Dirac node with linear energy dispersion (left). Each achiral fourfold Dirac node transforms into two doubly-degenerate chiral Weyl fermions with opposite chiral charges by breaking the P or Θ symmetry (right). c) Dirac or Weyl fermions trace a loop or line in materials with robust planer symmetries and form Dirac or Weyl nodal-line semimetals. d) Quadratic energy dispersion of double-Weyl fermions with chiral charge $C = |2|$. Here, two single-Weyl fermions with the same chiral charge merge on a rotational axis to generate a double-Weyl fermion. e) A threefold (spin 1) excitation and f) a fourfold (spin 3/2) Rarita–Schwinger–Weyl fermion. Realization of single-Weyl fermions in prototypical Weyl semimetal TaAs. g) The body-centered tetragonal crystal lattice of TaAs without inversion symmetry. h) Theoretically obtained distribution of nodal crossings in the bulk BZ without (black lines) and with (red and blue dots) spin-orbit coupling. The four nodal rings located on the $k_x = 0$ and $k_y = 0$ mirror planes are obtained in the absence of spin-orbit coupling. These nodal lines reduce to 12 pairs of single-Weyl fermions (W1 and W2) when the SOC is included. The red and blue dots distinguish between the opposite charges of the various Weyl fermions. i) Computed Fermi surface of Weyl fermions projected on the (001) surface BZ (white and black dots). j) Measured ARPES maps of Fermi arcs and the Weyl fermion nodes in TaAs. Fermi arcs emanating and terminating at Weyl fermion projections attest to the nontrivial topological phase of TaAs. Panels (g–j) reprinted with permission from Ref. [89], AAAS.

a 2D Chern insulator with a nonvanishing Chern number and chiral edge states. Chiral edge states of such 2D Chern insulators form open surface states in Weyl semimetals, which differ sharply from the conventional surface states with closed contours in crystals.[4,7] The number and nature of the Fermi arcs depend on the chiral charge of the Weyl nodes. Protected by lattice symmetries, the Weyl nodes in the multifold-fermion semimetals can support high values of the chiral charge unlike the Weyl fermions in high-energy physics as shown in Figure 2b–f. In Dirac semimetals, the two doubly-degenerate, oppositely charged Weyl nodes coalesce at the same momentum and energy point to realize a fourfold degenerate Dirac node. For this reason, Dirac semimetals host double-Fermi-arc surface states that have been observed in experiments.[89]

Dirac and Weyl semimetals differ in their lattice symmetries, which enforce degeneracies in electronic states. Under combined time-reversal and inversion symmetries, electronic bands must be at least two-fold spin degenerate at all k points as dictated by the Kramers' theorem ($E_{k\uparrow} = E_{k\downarrow}$). Both the time-reversal and inversion symmetries are preserved in Dirac semimetals and thus twofold degenerate bands can cross at specific k points to realize the fourfold Dirac nodes, see Figure 2b. Additional crystalline symmetries are needed to protect the Dirac nodes that would otherwise hybridize to open a gap at the crossing points. Dirac semimetals are identified as band-inversion-induced or symmetry-enforced depending on their formation mechanism. Band topology of the band-inversion driven Dirac semimetals is encoded in their high-order hinge states as surmised recently.[105] Dirac semimetals can be transformed into Weyl semimetals by breaking either the inversion or the time-reversal symmetry, which results in splitting each Dirac node into two chiral Weyl nodes. These Weyl nodes usually lie at generic k points in the BZ and remain intact as long as the translational symmetry is preserved. Weyl nodes can only be annihilated in pairs to achieve a topological phase transition to an insulating state[92] (Figure 2).

Fermions in condensed matter physics only respect the crystalline space-group symmetries, which are much lower than those of the Poincare group in high-energy physics.[106,107] The reduced symmetry constraints in crystals allow new types of Dirac and Weyl fermionic excitations that are not possible in the domain of high-energy physics. By examining the nature of the band crossings in the presence of rotational and mirror symmetries, higher charge double-Weyl fermions,[108,109] single-threefold and double-sixfold spin-1 Weyl fermions,[110–113] Kramers–Weyl fermions,[114] nexus fermions,[115,116] eightfold double-Dirac fermions,[117] and nodal-line fermions[118–122] that have no high-energy analog have been identified. Importantly, the spin-1 and spin-3/2 massless fermions beyond the putative spin-1/2 Weyl fermions have been realized in Chiral crystals with nonsymmorphic lattice symmetries as shown in Figure 2e–f. Fermionic excitations can be further classified as type I or type II depending on the degree to which the Lorentz symmetry is broken in the material.[121,122] Type I Weyl fermions host a conical energy dispersion with a point-like Fermi surface. In the type II case, we have a tilted energy dispersion, and the associated fermions exist at the touching points between the electron and hole Fermi pockets and induce highly directional responses in materials.[121,122]

Topological semimetals can also be characterized via the dimensionality of their band-touching points in the bulk BZ. Dirac, Weyl, and higher-fold fermions constitute zero-dimensional (0D) band-touching points in the momentum space. These band-touching points can become extended to form 1D nodal lines, which can be closed rings or open lines that run across the neighboring BZs. Multiple 1D nodal lines can cross each other to generate nontrivial links such as the Hopf links or coupled chains enabled by various planer symmetries.[119,120] Mirror-planes or a combination of time-reversal and inversion symmetries protect the nodal lines without the SOC, whereas only the mirror planes protect them with SOC.[85] The nodal lines (without SOC) may be viewed as the parents that spawn other topological phases when the SOC is included. Nodal lines in materials that do not respect time-reversal symmetries are usually twofold degenerate and the associated topological index is the winding number. Nodal-line semimetals exhibit drumhead surface states that connect the projections of bulk nodal lines over the surface BZ.[2–4] The 2D band-touching points forming nodal surfaces have been observed.[123,124]

Using first-principles predictive theoretical modeling combined with various experimental probes, many materials have been verified to host a variety of topological semimetallic states.[4] Examples include Dirac states in Na_3Bi,[89,96,97] Cd_3As_2,[98,99] KZnBi,[100] and transition-metal dichalcogenides,[101] Weyl fermions in nonmagnetic TaAs family, $Mo_xW_{1-x}Te_2$,[4] LaAlGe[122] and $TaIrTe_4$,[125] and the magnetic Heuslers,[119,126–128] $Co_3Sn_2S_2$,[129] and the (Ce,Pr)Al(Si,Ge) materials.[130,131] Nexus fermions in MoP,[132,133] high-fold Weyl fermions in the RhSi family,[110,111] and nodal fermions in the ZrSiS family,[134,135] $PbTaSe_2$,[136] and Co_2MnGa materials[128] have also been reported. Weyl fermion states driven by external electric and magnetic fields have been reported in GdPtBi,[137] TbPtBi,[138] and EuB_6.[139]

5. New frontiers in topological research

We now turn to comment on a few major emerging directions that we expect to grow in prominence over the coming years as we unravel new functionalities and the associated nontrivial science of topological materials (see **Figure 3**).

5.1. Robust Characterizations of Topological States

Considerable progress has been made toward characterizing topological states involving new types of quasiparticles and identifying the related candidate materials, especially in the nonmagnetic materials space. Symmetry indicators, which are based on the symmetries of the atomic lattices, have facilitated the identification of topological states in high-throughput calculations.[34–36] Such searches, however, often involve average high-symmetry configurations of materials, which may not be amenable to experimental realization.[140,141] Accurate first-principles computations can, therefore, be expected to continue to play a key role in identifying the most promising candidate materials. Moving forward, thermodynamical stability and effects of symmetry-breaking via charge, orbital or

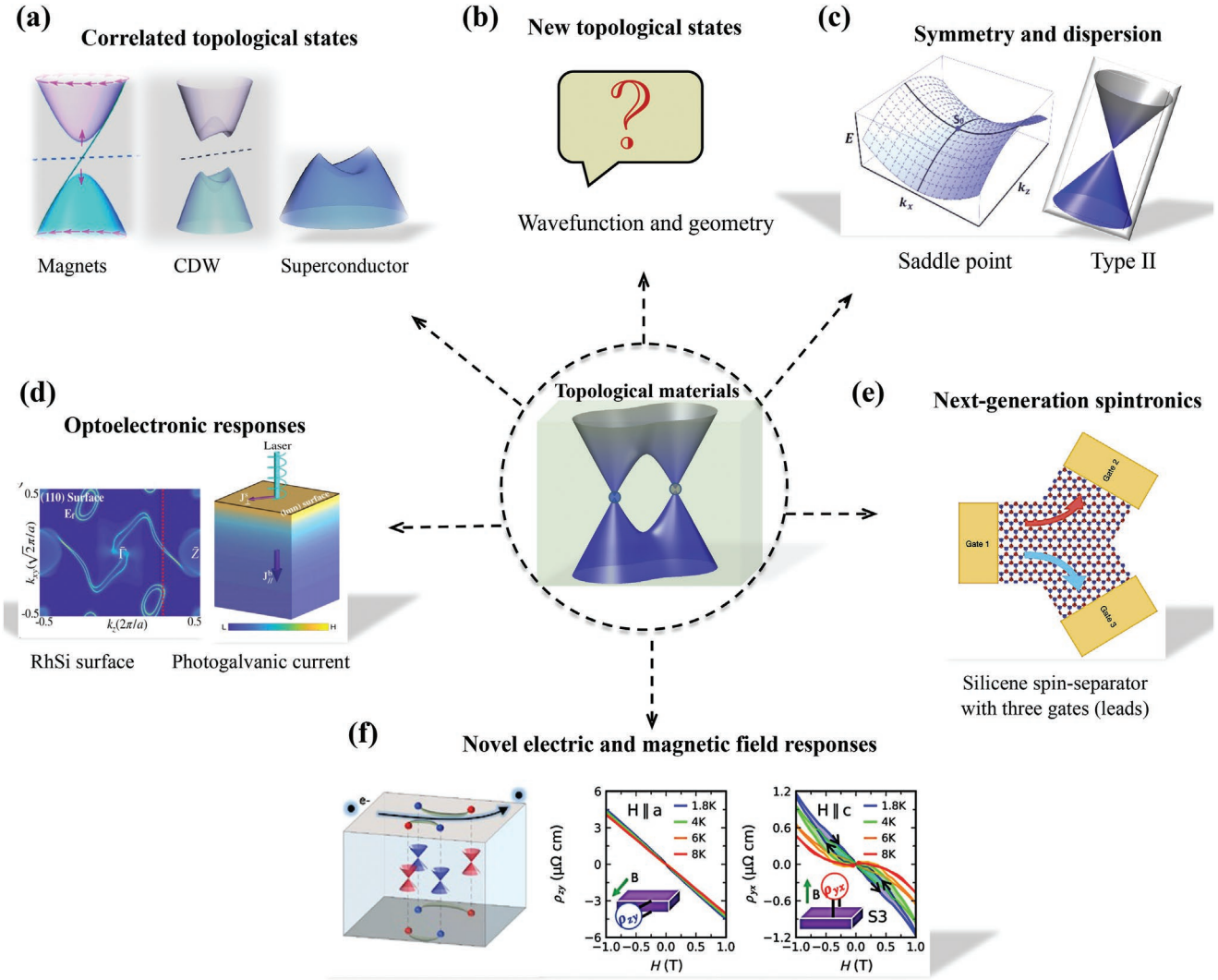

Figure 3. Landscape of topological research opportunities. Low-energy excitations enshrined in the Dirac and Weyl fermions are at the heart of the science, engineering and applications of topological materials (center; Weyl fermions are depicted). a) Topological order and strong electronic correlations drive correlated topological states in magnets, charge density wave (CDW) materials, and superconductors. b) New topological phases with novel responses can emerge through interactions involving spin, lattice, charge, and orbital degrees of freedom in quantum materials. c) Structural parameters and crystalline symmetries over the boundary surfaces/edges shape the nature, number, and dispersion of nontrivial states. Emergence of saddle-points and type II Weyl cones is highlighted. d) Topological materials can exhibit extreme optoelectronic responses. Theoretical results for the photogalvanic current in the chiral semimetal RhSi are shown. Photogalvanic current (left) flows perpendicular to the direction of the bulk injection current (right). e) Topological materials host protected spin-transport, which makes them appealing for next-generation spintronics devices. Design concept for a three-terminal gated silicene (one-atom-thick 2D hexagonal silicon) spin-separator is shown, which could produce nearly 100% spin-polarized currents robust against weak disorder and edge imperfections. f) Topological magnets support exotic electromagnetic responses. Example of CeAlSi is shown, which exhibits an anomalous Hall effect that is anisotropic between the easy and hard magnetic axes (middle and right). CeAlSi also shows a new type of loop Hall effect (right) that emerges from the topological Fermi arcs located on the magnetic domain walls (left). Panels reprinted with permission (c) from Ref. [85], APS; (d) from Ref. [148], APS; (e) from Ref. [149], Springer Nature Limited; and (f) from Ref. [131], APS.

magnetic ordering, electron–electron interactions, and doping and defects would need to be incorporated in computational modeling for more robust characterizations of topological states in the materials discovery efforts.[140,141] In-depth material-specific computations for various lattice symmetries and atomic and magnetic configurations for a given material are often needed for making a headway in interpreting experimental results. For example, pristine $TlBiSe_2$ was predicted as a Z_2 TI with a large bulk energy gap.[47,51] Slab models with flat Se or Tl-terminated surfaces found the Dirac-cone states to coexist with the trivial dangling-bond surface states. However, photoemission measurements find only a single Dirac cone state without the presence of trivial surface states.[46] Further analysis reveals that the discrepancy between theory and experiment arises here because the translational invariance over the surface is broken in $TlBiSe_2$ to yield a stoichiometrically rough nonpolar surface. When a 2×2 structure with appropriately lowered symmetry is considered, the calculated surface dispersion is found to be in excellent agreement with the measured Dirac cones states in $TlBiSe_2$.[142] This case study highlights the importance of

considering local motifs in high-quality materials searches as well as for sharpened comparisons between theory and experiment.

5.2. Surface Symmetries and Atomic and Magnetic Structures

Effects of local surface symmetries and atomic and magnetic structures on dispersions and properties of nontrivial states deserve greater attention in topological research.[85,134,135,143–145] Even though, the existence of topological surface states is guaranteed by the nontrivial geometry of the bulk electronic states, details of their actual energy dispersions and the energy-momentum-space windows in which they lie, and even their topological character can be sensitive to the symmetries over the surface. Depending on the nature of the bulk states and the crystalline symmetries involved, topological surface states with a variety of energy dispersions and characters have been predicted. Examples include saddle-like states,[85,87] helicoid states,[143] Seifert states,[144] and linked-node states.[134,135,145] Notably, crystalline surfaces that lack rotational symmetry $C_{n;n>2}$ support saddle points in their dispersions,[85] which would generate van Hove singularities (VHSs) with diverging (logarithmic or higher-order) densities of states (Figure 3(c)). These VHSs may amplify electron correlation effects and drive quantum instabilities in the topological matrix involving the charge, lattice, and spin degrees of freedom. Investigations of topological materials in thin-film geometries are important for accessing such novel features of topological surface states.

5.3. Topological Magnets

Insulating and metallic topological magnets, where long-range electronic correlations shape the nontrivial states provide a fertile research direction.[29,30,128,137] Ideal topological magnets host nontrivial states at or near the Fermi energy, which can drive many exotic quantum phenomena.[146,147] Magnetic order in non-magnetic topological materials can be induced via doping with magnetic dopants or by placing the material in proximity of magnets in constrained geometries[6,76,146] even though these approaches are sensitive to growth conditions. Intrinsic topological magnets could be realized in stochiometric magnetic compounds that feature exchange-coupled magnetic ions by tuning the symmetry of the underlying crystal lattice.[79] Thin films of topological magnets could realize quantum anomalous Hall effects with high operating temperatures, and would be amenable to integration into functional heterostructures for exploring designer quantum phenomena.[80–83] For example, the recently discovered stochiometric layered $MnBi_{2n}Te_{3n+1}$ materials support a variety of topological states such as the axion insulator, ferromagnetic TI, exchange-coupling driven Weyl semimetal, and the QAHS, depending on their composition, and exhibit novel electromagnetic phenomena such as the layer Hall effect.[81–83] Accurate modeling of magnetic materials is important for pinpointing the nature of the topological states under specific magnetic orders. Advances in first-principles density-functional based modeling, symmetry analysis, low-energy models, and experiments are all needed to make a headway in understanding correlated topological states in materials.

5.4. Topological States and Collective Excitations

Interplay between topological states and various collective excitations provides opportunities for exploring new physics.[5,6] Recent theoretical work suggests the presence of nontrivial topological states in CDW materials and superconductors.[150–155] Mechanisms involved include low-energy flat bands in Kagome materials,[152,153] large electron–phonon couplings in the conventional superconductors,[156] and more complex interactions in the cuprates and other novel superconductors.[157] Conventional superconductors and CDW phases driven by electron-phonon interactions or Fermi surface nesting can often be described accurately using material-specific tight-binding Hamiltonians based on first-principles calculations and solving the anisotropic Migdal–Eliashberg equations.[158,159] Relatively little attention has been paid to nontrivial states associated with phononic, plasmonic, and other bosonic excitations.

5.5. Materials Discovery Strategies

Here, we comment on the materials discovery process toward finding ideal topological materials in which effects of the nontrivial states are dominant. The key for generating a topological state near the charge neutrality point is the presence of a band inversion driven via the SOC or crystal-field effects, the two effects being intertwined in materials.[41–49,160] Promising candidate materials are thus small bandgap insulators or metals that contain heavy elements from the lower part of the periodic table with large SOC and/or crystal-field splitting, see Ref. [2]. One should focus on isostructural and isovalent materials families as they provide flexibility with respect to chemical compositions, lattice parameters, and transport properties.[41–49,79,80] An illustrative example is the $SrIn_2As_2$ Zintl family that can realize a tapestry of nonmagnetic and magnetic topological states, which are amenable to manipulation via various external controls.[79] $SrIn_2As_2$ is a dual topological insulator with Z_2 = (1;000) and mirror Chern number $C_M = -1$. Its magnetic cousin $EuIn_2As_2$ is an axion insulator with $Z_4 = 2$.[77–79] Breaking the time-reversal symmetry via Eu doping in $Sr_{1-x}Eu_xIn_2As_2$ drives it into a higher order or topological crystalline insulator depending on the magnetic configuration.[79] An ideal Weyl-point semimetal with the minimal two Weyl nodes or a Weyl-nodal semimetal with a single nodal line can also be realized via an external magnetic field in $EuIn_2P_2$. A multitude of topological states is thus possible by varying composition and applying external fields in this materials family. A bottom-up approach for designing synthetic materials for engineering topological states with tailor-made properties is another materials discovery strategy.[161,162]

5.6. Nontrivial Responses and Applications

We conclude with a few comments on nontrivial responses of topological materials, which drive their potential applications, although this aspect of topological physics is not our focus in this article.[146–149,163–166] Examples are anomalous Hall effect in magnetic topological materials and spin Hall

effect in nonmagnetic topological materials, which could produce anomalous thermoelectric couplings and thermal Hall effects. A loop-shaped Hall effect that appears only when the Fermi level lies close to the Weyl nodes in CeAlSi is another example.[131] Inversion-symmetry-breaking Weyl semimetals are of particular interest for nonlinear optoelectronic phenomena that are enhanced by the Berry curvature singularities.[166] Second-order harmonic generation, shift currents, circular photogalvanic effect, and giant Faraday and Kerr effects have been observed in Weyl semimetals.[148,163–166] Electromagnetic responses in topological materials thus provide unique opportunities for uncovering and controlling topological features of the quantum matter.

5.7. Outlook

It is clear that topological materials have opened up unprecedented opportunities for exploring fundamental science questions and novel electromagnetic responses driven by the geometric properties of the crystalline electronic states. We expect the field to continue to grow vigorously for many years into the future.

Acknowledgements

The authors thank S. M. Huang, S. Mardanya, X. Zhou, and B. Ghosh for discussions and feedback. This work is supported by the Department of Atomic Energy of the Government of India under Project No. 12-R&D-TFR-5.10-0100. The work at Northeastern University was supported by the Air Force Office of Scientific Research under award number FA9550-20-1-0322, and it benefited from the computational resources of Northeastern University's Advanced Scientific Computation Center (ASCC) and the Discovery Cluster. H.L. acknowledges the support by the Ministry of Science and Technology (MOST) in Taiwan under grant number MOST 109-2112-M-001-014-MY3.

Conflict of Interest

The authors declare no conflict of interest.

Keywords

electronic structure, topological insulators, weyl and dirac semimetals

Received: January 31, 2022
Revised: August 13, 2022
Published online: November 22, 2022

[1] F. D. M. Haldane, *Rev. Mod. Phys.* **2017**, *89*, 040502.
[2] A. Bansil, H. Lin, T. Das, *Rev. Mod. Phys.* **2016**, *88*, 021004.
[3] J. Xiao, B. Yan, *Nat. Rev. Phys.* **2021**, *3*, 283.
[4] M. Z. Hasan, G. Chang, I. Belopolski, G. Bian, S.-Y. Xu, J.-X. Yin, *Nat. Rev. Mater.* **2021**, *6*, 784.
[5] M. Z. Hasan, C. L. Kane, *Rev. Mod. Phys.* **2010**, *82*, 3045.
[6] X.-L. Qi, S.-C. Zhang, *Rev. Mod. Phys.* **2011**, *83*, 1057.
[7] N. P. Armitage, E. J. Mele, A. Vishwanath, *Rev. Mod. Phys.* **2018**, *90*, 015001.
[8] F. Bloch, *Zeitschrift für Physik* **1929**, *52*, 555.
[9] P. Hohenberg, W. Kohn, *Phys. Rev.* **1964**, *136*, B864.
[10] W. Kohn, L. J. Sham, *Phys. Rev.* **1965**, *140*, A1133.
[11] R. M. Martin, *Electronic Structure: Basic Theory and Practical Methods*, Cambridge University Press, Cambridge, England **2004**.
[12] Y. Zhang, C. Lane, J. W. Furness, B. Barbiellini, J. P. Perdew, R. S. Markiewicz, A. Bansil, J. Sun, *Proc. Natl. Acad. Sci. USA* **2020**, *117*, 68.
[13] S. Chang, *Phys. Today* **2016**, *69*, 14.
[14] C. L. Kane, E. J. Mele, *Phys. Rev. Lett.* **2005**, *95*, 226801.
[15] B. A. Bernevig, S.-C. Zhang, *Phys. Rev. Lett.* **2006**, *96*, 106802.
[16] L. Fu, C. L. Kane, E. J. Mele, *Phys. Rev. Lett.* **2007**, *98*, 106803.
[17] L. Fu, C. L. Kane, *Phys. Rev. B* **2007**, *76*, 045302.
[18] F. D. M. Haldane, *Phys. Rev. Lett.* **1988**, *61*, 2015.
[19] D. J. Thouless, M. Kohmoto, M. P. Nightingale, M. den Nijs, *Phys. Rev. Lett.* **1982**, *49*, 405.
[20] H. C. Po, A. Vishwanath, H. Watanabe, *Nat. Commun.* **2017**, *8*, 50.
[21] B. Bradlyn, L. Elcoro, J. Cano, M. G. Vergniory, Z. Wang, C. Felser, M. I. Aroyo, B. A. Bernevig, *Nature* **2017**, *547*, 298.
[22] Z. Song, T. Zhang, Z. Fang, C. Fang, *Nat. Commun.* **2018**, *9*, 3530.
[23] R. Yu, X. L. Qi, A. Bernevig, Z. Fang, X. Dai, *Phys. Rev. B* **2011**, *84*, 075119.
[24] A. A. Soluyanov, D. Vanderbilt, *Phys. Rev. B* **2011**, *83*, 035108.
[25] K. v. Klitzing, G. Dorda, M. Pepper, *Phys. Rev. Lett.* **1980**, *45*, 494.
[26] J. E. Avron, D. Osadchy, R. Seiler, *Phys. Today* **2003**, *56*, 38.
[27] Y. Tokura, M. Kawasaki, N. Nagaosa, *Nat. Phys.* **2017**, *13*, 1056.
[28] D. Pesin, A. H. MacDonald, *Nat. Mater.* **2012**, *11*, 409.
[29] F. Wilczek, *Phys. Rev. Lett.* **1987**, *58*, 1799.
[30] D. M. Nenno, C. A. C. Garcia, J. Gooth, C. Felser, P. Narang, *Nat. Rev. Phys.* **2020**, *2*, 682.
[31] M. Franz, *Physics* **2008**, *1*, 36.
[32] X.-L. Qi, T. L. Hughes, S.-C. Zhang, *Phys. Rev. B* **2008**, *78*, 195424.
[33] F. Tang, H. C. Po, A. Vishwanath, X. Wan, *Nat. Phys.* **2019**, *15*, 470.
[34] T. Zhang, Y. Jiang, Z. Song, H. Huang, Y. He, Z. Fang, H. Weng, C. Fang, *Nature* **2019**, *566*, 475.
[35] M. G. Vergniory, L. Elcoro, C. Felser, N. Regnault, B. A. Bernevig, Z. Wang, *Nature* **2019**, *566*, 480.
[36] F. Tang, H. C. Po, A. Vishwanath, X. Wan, *Nature* **2019**, *566*, 486.
[37] H. Lin, T. Das, Y. J. Wang, L. A. Wray, S.-Y. Xu, M. Z. Hasan, A. Bansil, *Phys. Rev. B* **2013**, *87*, 121202.
[38] Y. Hatsugai, *Phys. Rev. B* **1993**, *48*, 11851.
[39] A. M. Essin, V. Gurarie, *Phys. Rev. B* **2011**, *84*, 125132.
[40] W. Kohn, *Phys. Rev.* **1964**, *133*, A171.
[41] B. A. Bernevig, T. L. Hughes, S.-C. Zhang, *Science* **2006**, *314*, 1757.
[42] L. B. Zhang, K. Chang, X. C. Xie, H. Buhmann, L. W. Molenkamp, *New J. Phys.* **2010**, *12*, 083058.
[43] Y. Xia, D. Qian, D. Hsieh, L. Wray, A. Pal, H. Lin, A. Bansil, D. Grauer, Y. S. Hor, R. J. Cava, M. Z. Hasan, *Nat. Phys.* **2009**, *5*, 398.
[44] D. Hsieh, Y. Xia, L. Wray, D. Qian, A. Pal, J. H. Dil, J. Osterwalder, F. Meier, G. Bihlmayer, C. L. Kane, Y. S. Hor, R. J. Cava, M. Z. Hasan, *Science* **2009**, *323*, 919.
[45] H. Zhang, C.-X. Liu, X.-L. Qi, X. Dai, Z. Fang, S.-C. Zhang, *Nat. Phys.* **2009**, *5*, 438.
[46] S.-Y. Xu, Y. Xia, L. A. Wray, D. Qian, S. Jia, J. H. Dil, F. Meier, J. Osterwalder, B. Slomski, H. Lin, R. J. Cava, M. Z. Hasan, *Science* **2011**, *332*, 560.
[47] H. Lin, R. S. Markiewicz, L. A. Wray, L. Fu, M. Z. Hasan, A. Bansil, *Phys. Rev. Lett.* **2010**, *105*, 036404.
[48] B. Singh, H. Lin, R. Prasad, A. Bansil, *Phys. Rev. B* **2013**, *88*, 195147.
[49] B. Singh, H. Lin, R. Prasad, A. Bansil, *J. Appl. Phys.* **2014**, *116*, 033704.
[50] M. V. Berry, *Proc. R. Soc. Lond. A* **1984**, *392*, 45.
[51] B. Singh, A. Sharma, H. Lin, M. Z. Hasan, R. Prasad, A. Bansil, *Phys. Rev. B* **2012**, *86*, 115208.

[52] S. V. Eremeev, G. Landolt, T. V. Menshchikova, B. Slomski, Y. M. Koroteev, Z. S. Aliev, M. B. Babanly, J. Henk, A. Ernst, L. Patthey, A. Eich, A. A. Khajetoorians, J. Hagemeister, O. Pietzsch, J. Wiebe, R. Wiesendanger, P. M. Echenique, S. S. Tsirkin, I. R. Amiraslanov, J. H. Dil, E. V. Chulkov, *Nat. Commun.* **2012**, *3*, 635.
[53] H. Lin, L. A. Wray, Y. Xia, S. Xu, S. Jia, R. J. Cava, A. Bansil, M. Z. Hasan, *Nat. Mater.* **2010**, *9*, 546.
[54] S. Chadov, X. Qi, J. Kübler, G. H. Fecher, C. Felser, *Nat. Mater.* **2010**, *9*, 541.
[55] M. Dzero, K. Sun, V. Galitski, P. Coleman, *Phys. Rev. Lett.* **2010**, *104*, 106408.
[56] F. Lu, J. Zhao, H. Weng, Z. Fang, X. Dai, *Phys. Rev. Lett.* **2013**, *110*, 096401.
[57] S. Liu, Y. Kim, L. Z. Tan, A. M. Rappe, *Nano Lett.* **2016**, *16*, 1663.
[58] J.-J. Zhang, D. Zhu, B. I. Yakobson, *Nano Lett.* **2021**, *21*, 785.
[59] L. Fu, C. L. Kane, *Phys. Rev. Lett.* **2008**, *100*, 096407.
[60] Y. S. Hor, A. J. Williams, J. G. Checkelsky, P. Roushan, J. Seo, Q. Xu, H. W. Zandbergen, A. Yazdani, N. P. Ong, R. J. Cava, *Phys. Rev. Lett.* **2010**, *104*, 057001.
[61] P. Tang, B. Yan, W. Cao, S.-C. Wu, C. Felser, W. Duan, *Phys. Rev. B* **2014**, *89*, 041409.
[62] R. Noguchi, T. Takahashi, K. Kuroda, M. Ochi, T. Shirasawa, M. Sakano, C. Bareille, M. Nakayama, M. D. Watson, K. Yaji, A. Harasawa, H. Iwasawa, P. Dudin, T. K. Kim, M. Hoesch, V. Kandyba, A. Giampietri, A. Barinov, S. Shin, R. Arita, T. Sasagawa, T. Kondo, *Nature* **2019**, *566*, 518.
[63] L. Fu, *Phys. Rev. Lett.* **2011**, *106*, 106802.
[64] T. H. Hsieh, H. Lin, J. Liu, W. Duan, A. Bansil, L. Fu, *Nat. Commun.* **2012**, *3*, 982.
[65] X. Zhou, C.-H. Hsu, T.-R. Chang, H.-J. Tien, Q. Ma, P. Jarillo-Herrero, N. Gedik, A. Bansil, V. M. Pereira, S.-Y. Xu, H. Lin, L. Fu, *Phys. Rev. B* **2018**, *98*, 241104.
[66] C. Fang, L. Fu, *Sci. Adv.* **2019**, *5*, eaat2374.
[67] Y. Tanaka, Z. Ren, T. Sato, K. Nakayama, S. Souma, T. Takahashi, K. Segawa, Y. Ando, *Nat. Phys.* **2012**, *8*, 800.
[68] S.-Y. Xu, C. Liu, N. Alidoust, M. Neupane, D. Qian, I. Belopolski, J. D. Denlinger, Y. J. Wang, H. Lin, L. A. Wray, G. Landolt, B. Slomski, J. H. Dil, A. Marcinkova, E. Morosan, Q. Gibson, R. Sankar, F. C. Chou, R. J. Cava, A. Bansil, M. Z. Hasan, *Nat. Commun.* **2012**, *3*, 1192.
[69] A. Maiti, R. P. Pandeya, B. Singh, K. K. Iyer, A. Thamizhavel, K. Maiti, *Phys. Rev. B* **2021**, *104*, 195403.
[70] W. Fan, S. Nie, C. Wang, B. Fu, C. Yi, S. Gao, Z. Rao, D. Yan, J. Ma, M. Shi, Y. Huang, Y. Shi, Z. Wang, T. Qian, H. Ding, *Nat. Commun.* **2021**, *12*, 2052.
[71] J. Langbehn, Y. Peng, L. Trifunovic, F. von Oppen, P. W. Brouwer, *Phys. Rev. Lett.* **2017**, *119*, 246401.
[72] Z. Song, Z. Fang, C. Fang, *Phys. Rev. Lett.* **2017**, *119*, 246402.
[73] W. A. Benalcazar, B. A. Bernevig, T. L. Hughes, *Phys. Rev. B* **2017**, *96*, 245115.
[74] F. Schindler, A. M. Cook, M. G. Vergniory, Z. Wang, S. S. P. Parkin, B. A. Bernevig, T. Neupert, *Sci. Adv.* **2018**, *4*, eaat0346.
[75] Y. Tokura, K. Yasuda, A. Tsukazaki, *Nat. Rev. Phys.* **2019**, *1*, 126.
[76] C.-Z. Chang, J. Zhang, X. Feng, J. Shen, Z. Zhang, M. Guo, K. Li, Y. Ou, P. Wei, L.-L. Wang, Z.-Q. Ji, Y. Feng, S. Ji, X. Chen, J. Jia, X. Dai, Z. Fang, S.-C. Zhang, K. He, Y. Wang, L. Lu, X.-C. Ma, Q.-K. Xue, *Science* **2013**, *340*, 167.
[77] Y. Xu, Z. Song, Z. Wang, H. Weng, X. Dai, *Phys. Rev. Lett.* **2019**, *122*, 256402.
[78] S. Regmi, M. M. Hosen, B. Ghosh, B. Singh, G. Dhakal, C. Sims, B. Wang, F. Kabir, K. Dimitri, Y. Liu, A. Agarwal, H. Lin, D. Kaczorowski, A. Bansil, M. Neupane, *Phys. Rev. B* **2020**, *102*, 165153.
[79] A. B. Sarkar, S. Mardanya, S.-M. Huang, B. Ghosh, C.-Y. Huang, H. Lin, A. Bansil, T.-R. Chang, A. Agarwal, B. Singh, *Phys. Rev. Mater.* **2022**, *6*, 044204.
[80] J. Li, Y. Li, S. Du, Z. Wang, B.-L. Gu, S.-C. Zhang, K. He, W. Duan, Y. Xu, *Sci. Adv.* **2019**, *5*, eaaw5685.
[81] C. Hu, L. Ding, K. N. Gordon, B. Ghosh, H.-J. Tien, H. Li, A. G. Linn, S.-W. Lien, C.-Y. Huang, S. Mackey, J. Liu, P. V. S. Reddy, B. Singh, A. Agarwal, A. Bansil, M. Song, D. Li, S.-Y. Xu, H. Lin, H. Cao, T.-R. Chang, D. Dessau, N. Ni, *Sci. Adv.* **2020**, *6*, eaba4275.
[82] E. D. L. Rienks, S. Wimmer, J. Sánchez-Barriga, O. Caha, P. S. Mandal, J. Růžička, A. Ney, H. Steiner, V. V. Volobuev, H. Groiss, M. Albu, G. Kothleitner, J. Michalička, S. A. Khan, J. Minár, H. Ebert, G. Bauer, F. Freyse, A. Varykhalov, O. Rader, G. Springholz, *Nature* **2019**, *576*, 423.
[83] A. Gao, Y.-F. Liu, C. Hu, J.-X. Qiu, C. Tzschaschel, B. Ghosh, S.-C. Ho, D. Bérubé, R. Chen, H. Sun, Z. Zhang, X.-Y. Zhang, Y.-X. Wang, N. Wang, Z. Huang, C. Felser, A. Agarwal, T. Ding, H.-J. Tien, A. Akey, J. Gardener, B. Singh, K. Watanabe, T. Taniguchi, K. S. Burch, D. C. Bell, B. B. Zhou, W. Gao, H.-Z. Lu, A. Bansil, et al., *Nature* **2021**, *595*, 521.
[84] B. Wang, B. Singh, B. Ghosh, W.-C. Chiu, M. M. Hosen, Q. Zhang, L. Ying, M. Neupane, A. Agarwal, H. Lin, A. Bansil, *Phys. Rev. B* **2019**, *100*, 205118.
[85] B. Singh, X. Zhou, H. Lin, A. Bansil, *Phys. Rev. B* **2018**, *97*, 075125.
[86] B. Singh, S. Mardanya, C. Su, H. Lin, A. Agarwal, A. Bansil, *Phys. Rev. B* **2018**, *98*, 085122.
[87] B. Ghosh, S. Mardanya, B. Singh, X. Zhou, B. Wang, T.-R. Chang, C. Su, H. Lin, A. Agarwal, A. Bansil, *Phys. Rev. B* **2019**, *100*, 235101.
[88] A. H. Castro Neto, F. Guinea, N. M. R. Peres, K. S. Novoselov, A. K. Geim, *Rev. Mod. Phys.* **2009**, *81*, 109.
[89] S.-Y. Xu, I. Belopolski, N. Alidoust, M. Neupane, G. Bian, C. Zhang, R. Sankar, G. Chang, Z. Yuan, C.-C. Lee, S.-M. Huang, H. Zheng, J. Ma, D. S. Sanchez, B. Wang, A. Bansil, F. Chou, P. P. Shibayev, H. Lin, S. Jia, M. Z. Hasan, *Science* **2015**, *349*, 613.
[90] S. Murakami, *New J. Phys.* **2007**, *9*, 356.
[91] X. Wan, A. M. Turner, A. Vishwanath, S. Y. Savrasov, *Phys. Rev. B* **2011**, *83*, 205101.
[92] S.-M. Huang, S.-Y. Xu, I. Belopolski, C.-C. Lee, G. Chang, B. Wang, N. Alidoust, G. Bian, M. Neupane, C. Zhang, S. Jia, A. Bansil, H. Lin, M. Z. Hasan, *Nat. Commun.* **2015**, *6*, 7373.
[93] H. Weng, C. Fang, Z. Fang, B. A. Bernevig, X. Dai, *Phys. Rev. X* **2015**, *5*, 011029.
[94] B. Q. Lv, H. M. Weng, B. B. Fu, X. P. Wang, H. Miao, J. Ma, P. Richard, X. C. Huang, L. X. Zhao, G. F. Chen, Z. Fang, X. Dai, T. Qian, H. Ding, *Phys. Rev. X* **2015**, *5*, 031013.
[95] S. M. Young, S. Zaheer, J. C. Y. Teo, C. L. Kane, E. J. Mele, A. M. Rappe, *Phys. Rev. Lett.* **2012**, *108*, 140405.
[96] Z. Wang, Y. Sun, X.-Q. Chen, C. Franchini, G. Xu, H. Weng, X. Dai, Z. Fang, *Phys. Rev. B* **2012**, *85*, 195320.
[97] Z. K. Liu, B. Zhou, Y. Zhang, Z. J. Wang, H. M. Weng, D. Prabhakaran, S.-K. Mo, Z. X. Shen, Z. Fang, X. Dai, Z. Hussain, Y. L. Chen, *Science* **2014**, *343*, 864.
[98] M. Neupane, S.-Y. Xu, R. Sankar, N. Alidoust, G. Bian, C. Liu, I. Belopolski, T.-R. Chang, H.-T. Jeng, H. Lin, A. Bansil, F. Chou, M. Z. Hasan, *Nat. Commun.* **2014**, *5*, 3786.
[99] S. Borisenko, Q. Gibson, D. Evtushinsky, V. Zabolotnyy, B. Büchner, R. J. Cava, *Phys. Rev. Lett.* **2014**, *113*, 027603.
[100] J. Song, S. Kim, Y. Kim, H. Fu, J. Koo, Z. Wang, G. Lee, J. Lee, S. H. Oh, J. Bang, T. Matsushita, N. Wada, H. Ikegami, J. D. Denlinger, Y. H. Lee, B. Yan, Y. Kim, S. W. Kim, *Phys. Rev. X* **2021**, *11*, 021065.
[101] M. S. Bahramy, O. J. Clark, B.-J. Yang, J. Feng, L. Bawden, J. M. Riley, I. Markovic, F. Mazzola, V. Sunko, D. Biswas, S. P. Cooil, M. Jorge, J. W. Wells, M. Leandersson, T. Balasubramanian, J. Fujii, I. Vobornik, J. E. Rault, T. K. Kim, M. Hoesch, K. Okawa, M. Asakawa, T. Sasagawa, T. Eknapakul, W. Meevasana, P. D. C. King, *Nat. Mater.* **2018**, *17*, 21.
[102] D. P. A. Maurice, *Proc. R. Soc. Lond. A* **1928**, *117*, 610.

[103] H. Weyl, *Zeitschrift für Physik* **1929**, *56*, 330.
[104] H. Nielsen, M. Ninomiya, *Phys. Lett. B* **1983**, *130*, 389.
[105] B. J. Wieder, Z. Wang, J. Cano, X. Dai, L. M. Schoop, B. Bradlyn, B. A. Bernevig, *Nat. Commun.* **2020**, *11*, 627.
[106] M. H. Poincaré, *Rendiconti del Circolo Matematico di Palermo (1884-1940)* **1906**, *21*, 129.
[107] B. Bradlyn, J. Cano, Z. Wang, M. G. Vergniory, C. Felser, R. J. Cava, B. A. Bernevig, *Science* **2016**, *353*, aaf5037.
[108] S.-M. Huang, S.-Y. Xu, I. Belopolski, C.-C. Lee, G. Chang, T.-R. Chang, B. Wang, N. Alidoust, G. Bian, M. Neupane, D. Sanchez, H. Zheng, H.-T. Jeng, A. Bansil, T. Neupert, H. Lin, M. Z. Hasan, *Proc. Natl. Acad. Sci. USA* **2016**, *113*, 1180.
[109] B. Singh, G. Chang, T.-R. Chang, S.-M. Huang, C. Su, M.-C. Lin, H. Lin, A. Bansil, *Sci. Rep.* **2018**, *8*, 10540.
[110] G. Chang, S.-Y. Xu, B. J. Wieder, D. S. Sanchez, S.-M. Huang, I. Belopolski, T.-R. Chang, S. Zhang, A. Bansil, H. Lin, M. Z. Hasan, *Phys. Rev. Lett.* **2017**, *119*, 206401.
[111] P. Tang, Q. Zhou, S.-C. Zhang, *Phys. Rev. Lett.* **2017**, *119*, 206402.
[112] D. S. Sanchez, I. Belopolski, T. A. Cochran, X. Xu, J.-X. Yin, G. Chang, W. Xie, K. Manna, V. Süß, C.-Y. Huang, N. Alidoust, D. Multer, S. S. Zhang, N. Shumiya, X. Wang, G.-Q. Wang, T.-R. Chang, C. Felser, S.-Y. Xu, S. Jia, H. Lin, M. Z. Hasan, *Nature* **2019**, *567*, 500.
[113] Z. Rao, H. Li, T. Zhang, S. Tian, C. Li, B. Fu, C. Tang, L. Wang, Z. Li, W. Fan, J. Li, Y. Huang, Z. Liu, Y. Long, C. Fang, H. Weng, Y. Shi, H. Lei, Y. Sun, T. Qian, H. Ding, *Nature* **2019**, *567*, 496.
[114] G. Chang, B. J. Wieder, F. Schindler, D. S. Sanchez, I. Belopolski, S.-M. Huang, B. Singh, D. Wu, T.-R. Chang, T. Neupert, S.-Y. Xu, H. Lin, M. Z. Hasan, *Nat. Mater.* **2018**, *17*, 978.
[115] G. Chang, S.-Y. Xu, S.-M. Huang, D. S. Sanchez, C.-H. Hsu, G. Bian, Z.-M. Yu, I. Belopolski, N. Alidoust, H. Zheng, T.-R. Chang, H.-T. Jeng, S. A. Yang, T. Neupert, H. Lin, M. Z. Hasan, *Sci. Rep.* **2017**, *7*, 1688.
[116] S. Mardanya, B. Singh, S.-M. Huang, T.-R. Chang, C. Su, H. Lin, A. Agarwal, A. Bansil, *Phys. Rev. Mater.* **2019**, *3*, 071201.
[117] B. J. Wieder, Y. Kim, A. M. Rappe, C. L. Kane, *Phys. Rev. Lett.* **2016**, *116*, 186402.
[118] A. A. Burkov, M. D. Hook, L. Balents, *Phys. Rev. B* **2011**, *235126*, 1.
[119] G. Chang, S.-Y. Xu, X. Zhou, S.-M. Huang, B. Singh, B. Wang, I. Belopolski, J. Yin, S. Zhang, A. Bansil, H. Lin, M. Z. Hasan, *Phys. Rev. Lett.* **2017**, *119*, 156401.
[120] B. Singh, B. Ghosh, C. Su, H. Lin, A. Agarwal, A. Bansil, *Phys. Rev. Lett.* **2018**, *121*, 226401.
[121] A. A. Soluyanov, D. Gresch, Z. Wang, Q. Wu, M. Troyer, X. Dai, B. A. Bernevig, *Nature* **2015**, *527*, 495.
[122] S.-Y. Xu, N. Alidoust, G. Chang, H. Lu, B. Singh, I. Belopolski, D. S. Sanchez, X. Zhang, G. Bian, H. Zheng, M.-A. Husanu, Y. Bian, S.-M. Huang, C.-H. Hsu, T.-R. Chang, H.-T. Jeng, A. Bansil, T. Neupert, V. N. Strocov, H. Lin, S. Jia, M. Z. Hasan, *Sci. Adv.* **2017**, *3*, e1603266.
[123] W. Wu, Y. Liu, S. Li, C. Zhong, Z.-M. Yu, X.-L. Sheng, Y. X. Zhao, S. A. Yang, *Phys. Rev. B* **2018**, *97*, 115125.
[124] R. Zhang, C.-Y. Huang, J. Kidd, R. S. Markiewicz, H. Lin, A. Bansil, B. Singh, J. Sun, *Phys. Rev. B* **2022**, *105*, 165140.
[125] I. Belopolski, P. Yu, D. S. Sanchez, Y. Ishida, T.-R. Chang, S. S. Zhang, S.-Y. Xu, H. Zheng, G. Chang, G. Bian, H.-T. Jeng, T. Kondo, H. Lin, Z. Liu, S. Shin, M. Z. Hasan, *Nat. Commun.* **2017**, *8*, 942.
[126] G. Chang, S.-Y. Xu, H. Zheng, B. Singh, C.-H. Hsu, G. Bian, N. Alidoust, I. Belopolski, D. S. Sanchez, S. Zhang, H. Lin, M. Z. Hasan, *Sci. Rep.* **2016**, *6*, 38839.
[127] Z. Wang, M. G. Vergniory, S. Kushwaha, M. Hirschberger, E. V. Chulkov, A. Ernst, N. P. Ong, R. J. Cava, B. A. Bernevig, *Phys. Rev. Lett.* **2016**, *117*, 236401.
[128] I. Belopolski, K. Manna, D. S. Sanchez, G. Chang, B. Ernst, J. Yin, S. S. Zhang, T. Cochran, N. Shumiya, H. Zheng, B. Singh, G. Bian, D. Multer, M. Litskevich, X. Zhou, S.-M. Huang, B. Wang, T.-R. Chang, S.-Y. Xu, A. Bansil, C. Felser, H. Lin, M. Z. Hasan, *Science* **2019**, *365*, 1278.
[129] D. F. Liu, A. J. Liang, E. K. Liu, Q. N. Xu, Y. W. Li, C. Chen, D. Pei, W. J. Shi, S. K. Mo, P. Dudin, T. Kim, C. Cacho, G. Li, Y. Sun, L. X. Yang, Z. K. Liu, S. S. P. Parkin, C. Felser, Y. L. Chen, *Science* **2019**, *365*, 1282.
[130] G. Chang, B. Singh, S.-Y. Xu, G. Bian, S.-M. Huang, C.-H. Hsu, I. Belopolski, N. Alidoust, D. S. Sanchez, H. Zheng, H. Lu, X. Zhang, Y. Bian, T.-R. Chang, H.-T. Jeng, A. Bansil, H. Hsu, S. Jia, T. Neupert, H. Lin, M. Z. Hasan, *Phys. Rev. B* **2018**, *97*, 041104.
[131] H.-Y. Yang, B. Singh, J. Gaudet, B. Lu, C.-Y. Huang, W.-C. Chiu, S.-M. Huang, B. Wang, F. Bahrami, B. Xu, J. Franklin, I. Sochnikov, D. E. Graf, G. Xu, Y. Zhao, C. M. Hoffman, H. Lin, D. H. Torchinsky, C. L. Broholm, A. Bansil, F. Tafti, *Phys. Rev. B* **2021**, *103*, 115143.
[132] Z. Zhu, G. W. Winkler, Q. Wu, J. Li, A. A. Soluyanov, *Phys. Rev. X* **2016**, *6*, 031003.
[133] G. Chang, S.-Y. Xu, S.-M. Huang, D. S. Sanchez, C.-H. Hsu, G. Bian, Z.-M. Yu, I. Belopolski, N. Alidoust, H. Zheng, T.-R. Chang, H.-T. Jeng, S. A. Yang, T. Neupert, H. Lin, M. Z. Hasan, *Sci. Rep.* **2017**, *7*, 1688.
[134] L. M. Schoop, M. N. Ali, C. Straßer, A. Topp, A. Varykhalov, D. Marchenko, V. Duppel, S. S. P. Parkin, B. V. Lotsch, C. R. Ast, *Nat. Commun.* **2016**, *7*, 11696.
[135] M. S. Lodge, G. Chang, C.-Y. Huang, B. Singh, J. Hellerstedt, M. T. Edmonds, D. Kaczorowski, M. M. Hosen, M. Neupane, H. Lin, M. S. Fuhrer, B. Weber, M. Ishigami, *Nano Lett.* **2017**, *17*, 7213.
[136] G. Bian, T.-R. Chang, R. Sankar, S.-Y. Xu, H. Zheng, T. Neupert, C.-K. Chiu, S.-M. Huang, G. Chang, I. Belopolski, D. S. Sanchez, M. Neupane, N. Alidoust, C. Liu, B. Wang, C.-C. Lee, H.-T. Jeng, C. Zhang, Z. Yuan, S. Jia, A. Bansil, F. Chou, H. Lin, M. Z. Hasan, *Nat. Commun.* **2016**, *7*, 10556.
[137] C. Shekhar, N. Kumar, V. Grinenko, S. Singh, R. Sarkar, H. Luetkens, S.-C. Wu, Y. Zhang, A. C. Komarek, E. Kampert, Y. Skourski, J. Wosnitza, W. Schnelle, A. McCollam, U. Zeitler, J. Kübler, B. Yan, H.-H. Klauss, S. S. P. Parkin, C. Felser, *Proc. Natl. Acad. Sci. USA* **2018**, *115*, 9140.
[138] Y. Zhu, B. Singh, Y. Wang, C.-Y. Huang, W.-C. Chiu, B. Wang, D. Graf, Y. Zhang, H. Lin, J. Sun, A. Bansil, Z. Mao, *Phys. Rev. B* **2020**, *101*, 161105.
[139] S.-Y. Gao, S. Xu, H. Li, C.-J. Yi, S.-M. Nie, Z.-C. Rao, H. Wang, Q.-X. Hu, X.-Z. Chen, W.-H. Fan, J.-R. Huang, Y.-B. Huang, N. Pryds, M. Shi, Z.-J. Wang, Y.-G. Shi, T.-L. Xia, T. Qian, H. Ding, *Phys. Rev. X* **2021**, *11*, 021016.
[140] A. Zunger, *Nature* **2019**, *566*, 447.
[141] O. I. Malyi, A. Zunger, *Appl. Phys. Rev.* **2020**, *7*, 041310.
[142] B. Singh, H. Lin, R. Prasad, A. Bansil, *Phys. Rev. B* **2016**, *93*, 085113.
[143] C. Fang, L. Lu, J. Liu, L. Fu, *Nat. Phys.* **2016**, *12*, 936.
[144] L. Li, C. H. Lee, J. Gong, *Commun. Phys.* **2019**, *2*, 135.
[145] B. Peng, S. Murakami, B. Monserrat, T. Zhang, *npj Computat. Mater.* **2021**, *7*, 195.
[146] N. Nagaosa, J. Sinova, S. Onoda, A. H. MacDonald, N. P. Ong, *Rev. Mod. Phys.* **2010**, *82*, 1539.
[147] D. Xiao, M.-C. Chang, Q. Niu, *Rev. Mod. Phys.* **2010**, *82*, 1959.
[148] G. Chang, J.-X. Yin, T. Neupert, D. S. Sanchez, I. Belopolski, S. S. Zhang, T. A. Cochran, Z. Chéng, M.-C. Hsu, S.-M. Huang, B. Lian, S.-Y. Xu, H. Lin, M. Z. Hasan, *Phys. Rev. Lett.* **2020**, *124*, 166404.
[149] W.-F. Tsai, C.-Y. Huang, T.-R. Chang, H. Lin, H.-T. Jeng, A. Bansil, *Nat. Commun.* **2013**, *4*, 1500.
[150] M.-C. Hsu, B. Singh, C.-H. Hsu, S.-Y. Xu, H. Lin, S.-M. Huang, *New J. Phys.* **2021**, *23*, 093025.

[151] S.-M. Huang, S.-Y. Xu, B. Singh, M.-C. Hsu, C.-H. Hsu, C. Su, A. Bansil, H. Lin, *New J. Phys.* **2021**, *23*, 083037.
[152] B. R. Ortiz, S. M. L. Teicher, Y. Hu, J. L. Zuo, P. M. Sarte, E. C. Schueller, A. M. M. Abeykoon, M. J. Krogstad, S. Rosenkranz, R. Osborn, R. Seshadri, L. Balents, J. He, S. D. Wilson, *Phys. Rev. Lett.* **2020**, *125*, 247002.
[153] X. Wu, T. Schwemmer, T. Müller, A. Consiglio, G. Sangiovanni, D. Di Sante, Y. Iqbal, W. Hanke, A. P. Schnyder, M. M. Denner, M. H. Fischer, T. Neupert, R. Thomale, *Phys. Rev. Lett.* **2021**, *127*, 177001.
[154] S. Ono, H. Watanabe, *Phys. Rev. B* **2018**, *98*, 115150.
[155] M. Geier, P. W. Brouwer, L. Trifunovic, *Phys. Rev. B* **2020**, *101*, 245128.
[156] K.-H. Jin, H. Huang, J.-W. Mei, Z. Liu, L.-K. Lim, F. Liu, *npj Comput. Mater.* **2019**, *5*, 57.
[157] A. Garg, M. Randeria, N. Trivedi, *Nat. Phys.* **2008**, *4*, 762.
[158] F. Giustino, *Rev. Mod. Phys.* **2017**, *89*, 015003.
[159] E. R. Margine, F. Giustino, *Phys. Rev. B* **2013**, *87*, 024505.
[160] J. Liu, X. Qian, L. Fu, *Nano Lett.* **2015**, *15*, 2657.
[161] Y.-L. Hong, Z. Liu, L. Wang, T. Zhou, W. Ma, C. Xu, S. Feng, L. Chen, M.-L. Chen, D.-M. Sun, X.-Q. Chen, H.-M. Cheng, W. Ren, *Science* **2020**, *369*, 670.
[162] R. Islam, B. Ghosh, C. Autieri, S. Chowdhury, A. Bansil, A. Agarwal, B. Singh, *Phys. Rev. B* **2021**, *104*, L201112.
[163] F. de Juan, A. G. Grushin, T. Morimoto, J. E. Moore, *Nat. Commun.* **2017**, *8*, 15995.
[164] Z. Z. Du, H.-Z. Lu, X. C. Xie, *Nat. Rev. Phys.* **2021**, *3*, 744.
[165] Q. L. He, T. L. Hughes, N. P. Armitage, Y. Tokura, K. L. Wang, *Nat. Mater.* **2022**, *21*, 15.
[166] Q. Ma, A. G. Grushin, K. S. Burch, *Nat. Mater.* **2021**, *20*, 1601.

Bahadur Singh is a Reader in the Department of Condensed Matter Physics and Materials Science at Tata Institute of Fundamental Research (TIFR) Mumbai. He is the Early Carrier Editorial Board member of the *Journal of Physics and Chemistry of Solids*. Bahadur received his Ph.D. degree from IIT Kanpur India in 2015. His research focuses on understanding the interplay between various quantum degrees of freedom and revealing anomalous properties and nontrivial science arising from their combinations in materials. He designed, predicted, and characterized many new classes of quantum materials ranging from topological materials to nanomaterials and superconductors.

Hsin Lin received the Ph.D. degree in physics from Northeastern University, Boston, MA, USA, in 2008. His research focuses on the electronic structure and spectroscopy of exotic quantum states of matter. Dr. Lin has discovered for the very first-time in the world several new classes of topological materials with novel theoretical calculations. He predicted Z_2 topological phases in Bi_2Se_3, $TlBiSe_2$, $GeBi_2Te_4$ family, and half-Heuslers as well as the first topological crystalline insulator in SnTe class. His theoretical prediction in 2015 that the TaAs class can host the Weyl fermions, launched an intense world-wide activity focused on these materials.

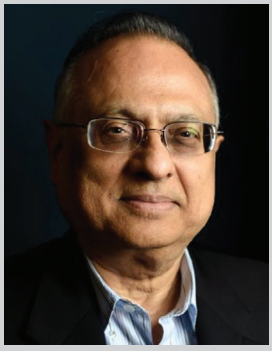

Arun Bansil is a University Distinguished Professor of physics at Northeastern University (NU). He is a Fellow of the American Physical Society, an academic editor of the *Journal of Physics and Chemistry of Solids* (1994-), and the Founding Director of NU's Advanced Scientific Computation Center (1999-). He managed the Theoretical Condensed Matter Physics program at the U.S.D.O.E (2008-10). He has authored/co-authored over 400 technical articles and edited 17 volumes of conference proceedings and a major book on *X-Ray Compton Scattering* (Oxford University Press, Oxford, 2004). Bansil is a Highly Cited Researcher (ISI Web of Science/Clarivate Analytics: 2017-2021, all years).